Phase separation in $Y_{1-x}Ca_xTiO_3$ associated with the insulator-to-metal transition: Observation by transmission electron microscopy

H. Matsuhata*

Nanoelectronics Research Institute, National Institute of Advanced Industrial Science and Technology, 1-1-1, Umezono, Tsukuba, 305-8568, Japan

F. Iga, M. Tsubota, T. Nakano, and T. Takabatake

Department of Quantum Matter, Graduate School of Advanced Sciences of Matter, Hiroshima University, Higashi-Hiroshima 739-8530, Japan

K. Kato

Japan Synchrotron Radiation Institute, Spring-8, 1-1-1 Kouto, Mikazuki-cho, Sayo-gun, Hyogo 679-5198, Japan

Structural changes in $Y_{1-x}Ca_xTiO_3$ ($x=0.37$, 0.39 and 0.41) during a transition from an insulator-to-metal were investigated by transmission electron microscopy. In a specimen for $x=0.39$, on cooling a transition from orthorhombic to monoclinic lattice was observed first. The onset of this transition was not certain, but the monoclinic lattice was clearly observed at 170 K. On further cooling to 140 K, approximately the metal-insulator transition temperature, an introduction of strain to this monoclinic phase was observed. Below 140 K a state of phase separation, with growth of domains, was observed. In the insulator specimen for $x=0.37$ the transition from orthorhombic to monoclinic lattice was observed similarly to the case of $x=0.39$, but no phase separation was observed in the range from room temperature to 110 K. In the case for $x=0.41$, the phase separation was also observed on cooling, but transition temperature of the phase separation is lower than that reported by x-ray diffraction. The phase separation observed presently for 0.39 and 0.41 is considered to be a kind of electrical phase separation, which drives the appearance of the metallic state at low temperatures. This is the first report on observation of separated domains on the electrical phase separation associated with the metal-insulator transition in paramagnetic $Y_{1-x}Ca_xTiO_3$.

I. INTRODUCTION

The metal-insulator (MI) transition induced by electron-electron interactions i.e., Mott transition has been investigated theoretically and experimentally for many years.[1] The transitional-metal oxide V_2O_3 is known as a typical example of the Mott insulator.[2] In this case a MI transition occurs in the paramagnetic region, though the low-temperature state is accompanied by a long-range antiferromagnetic ordering. The MI transition in the absence of magnetic ordering is one of the interesting issues. However, few examples of this type transition are reported.

In the system of $Y_{1-x}Ca_xTiO_3$, the MI transition is known to occur in the paramagnetic region. For many years this system has been investigated intensively.[3–10] Imada *et al.* reviewed recent experimental results on this system, see Sec. IV B.1 of Ref. 11. In $YTiO_3$, it is known that Ti-$3d^1$ electron energy level is split into two levels by the Hubbard gap. The gap between the unoccupied upper Hubbard band and the lower one is reported to be approximately 1 eV by optical conductivity.[6] Furthermore, the charge transfer gap between the unoccupied upper Hubbard band and the oxygen $2p$ band is approximately 4 eV.[10] This indicates that $YTiO_3$ is not the charge-transfer type insulator, but a Mott-Hubbard type.[12] $YTiO_3$ becomes ferromagnetic below 30 K. With increasing x in $Y_{1-x}Ca_xTiO_3$, the magnetic ordering disappears at $x \sim 0.12$, and the MI transition occurs around $x \sim 0.37–0.40$ in

the paramagnetic region. It has been a puzzle that the system remains an insulator up to around $x \sim 0.37–0.40$. Tokura *et al.* argued this to be a carrier localization effect arising from the combined effects of the electron correlation and random potential.[4–6] At $x \simeq 0.38–0.40$, a transition from the insulating state to the metallic state takes place on cooling at around 150 K without magnetic ordering.[3–6] This transition was found to be the first order type associated with significant hysteresis in both magnetic susceptibility and electrical resistivity.[13,14]

Recently, Kato *et al.*[15] have reported fine and subtle changes in x-ray diffraction pattern in the temperature region over the MI transition at $x \simeq 0.37–0.41$. In specimen for $x=0.39$ on cooling, a transition from insulator orthorhombic phase to insulator monoclinic phase takes place. Upon further cooling, at MI-transition temperature (T_{MI}) a new low temperature orthorhombic (LTO) phase appears. Below T_{MI}, a two-phase coexistent state, consisting of the monoclinic and LTO phase, is observed.

In order to investigate further details of nanostructure on phase separation, application of transmission electron microscope is expected to be appropriate, since sizes and shapes of separated domains, growth process, and such are possible to observe in real space. In this paper, we report on the results of structural observations by TEM in the temperature range from room temperature to 110 K, in the vicinity of the insulator-to-metal transition of $Y_{1-x}Ca_xTiO_3$ (x
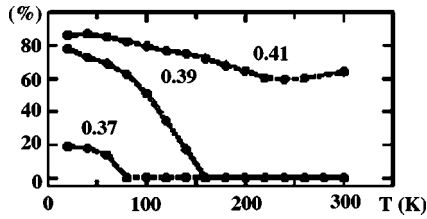
FIG. 1. Volume fraction of the low temperature orthorhombic (LTO) phase in the specimens for $x=0.37$, 0.39, and 0.41 of $Y_{1-x}Ca_xTiO_3$ obtained from the x-ray powder diffraction experiments. The LTO phase appears below the insulator-to-metal transition temperatures (T_{MI}), and the two-phase state with the monoclinic phase takes place. On further cooling the volume fraction of the LTO phase increases (Ref. 16).

$\simeq 0.37$–0.41). Some experimental results by x-ray diffraction are also described in order to compare to present results.

II. EXPERIMENT

Single crystals of $Y_{1-x}Ca_xTiO_3$ ($x=0.37$, 0.39, and 0.41) for TEM experiment were grown by the floating zone refinement technique, and powder specimens for x-ray diffraction were also prepared with the same synthesis procedure, see details in Ref. 16. At room temperature the specimen for $x=0.39$ adopts space group *Pbnm* (International table, No. 62), and $a=0.532$ nm, $b=0.554$ nm, $c=0.766$ nm. For the TEM experiments, thin film specimens were prepared by the mechanical polishing and ion milling. The specimens were observed at [100], [010] and [001] zone axes directions using a JEOL JEM-4000FX at accelerating voltages of 100 and 200 kV, to avoid radiation damage. In order to examine small differences in crystal lattice type, convergent beam electron diffraction patterns (see, for example, Ref. 17) were observed as well. A Gatan double tilt N_2 cooling holder was used for the observation down to 110 K. Before the TEM observations, an x-ray diffraction experiment was carried out with powdered specimens at BL02B2 in SPring8.

It is known[3–6,13–16] that the specimen for $x=0.37$ is an insulator at room temperature, and the transition to a metal takes place around 60 K. The one for $x=0.39$, the transition to a metal takes place around 150 K. The one for $x=0.41$ is a metal even at room temperature. In the specimens for $x=0.37$ and 0.39, the crystal lattice is an orthorhombic at room temperature. However, a phase transition to a monoclinic lattice takes place on cooling below 230 and 240 K, respectively. On further cooling, a new low temperature orthorhombic (LTO) phase appears at T_{MI}, and the two-phase separation state takes place in the metallic region.[15] In the specimen for $x=0.41$, the two-phase state is stable at room temperature.[15] Figure 1 shows volume fractions of the LTO phases in specimens for $x=0.37$, 0.39 and 0.41, which are obtained by powder x-ray diffraction.[15] The figure indicates the appearance of the LTO phase at T_{MI}, and increases in volume oncooling in the region of the two-phase state.

Similar results are obtained by present electron microscopic experiments. In the specimen for $x=0.39$, at room
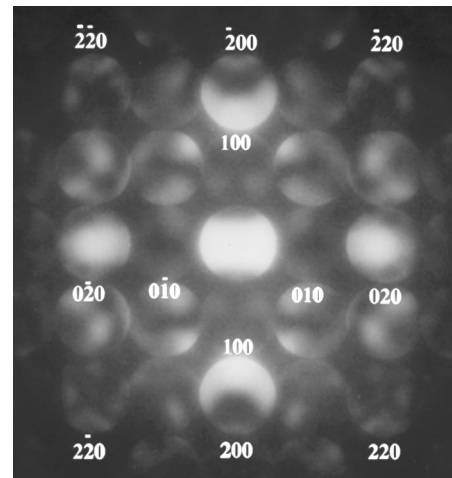

FIG. 2. CBED pattern taken at room temperature at the [001] zone axis of the specimen with $x=0.39$. Both horizontal and vertical mirror symmetries in the CBED pattern are observed.

temperature, a uniform state without any presence of microstructure is observed. On cooling, the change to the monoclinic phase is observed in CBED patterns as seen in Figs. 2 and 3. Here the CBED pattern was taken at the room temperature at the [001] zone axis direction, where horizontal and vertical symmetries are observed in the pattern. Figure 3 is an example of CBED pattern taken at 150 K at the [001] zone axis direction, where an absence of horizontal symmetry is observed. This asymmetry appears on reflections not only in the zeroth-order Laue zone, but also in higher-order zones for both [100] and [001] zone axes. This indicates the transition to the monoclinic lattice, i.e., the angle β (the angle between the *a*-axis direction and the *c*-axis direction) slightly changes from 90°. On cooling, this asymmetry is
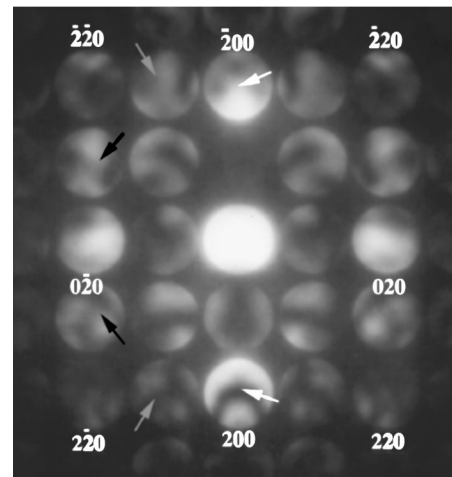

FIG. 3. CBED pattern taken at 150 K at the [001] zone axis direction of the specimen for $x=0.39$. Horizontal asymmetry in the pattern is observed, whereas the vertical mirror symmetry in the pattern is conserved. Arrows indicate example positions, where the absences in horizontal mirror symmetry in contrast are observed. This change in CBED pattern is due to the transition to a monoclinic lattice.
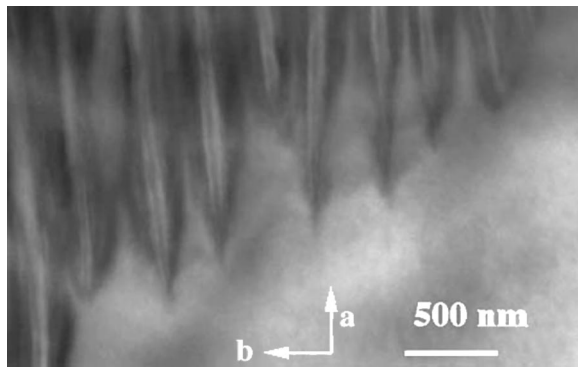
FIG. 4. The phase separated state observed at 110 K at the [001] zone axis direction of the specimen for $x=0.39$. The crystallographic a-axis direction and b-axis direction are indicated. The lower part is the monoclinic phase. The crystallographic type of lamella domains is uncertain, since the patterns in the CBED are distorted.

FIG. 5. Two kinds of domains observed at 110 K at the [010] zone axis direction of the specimen for $x=0.39$. The crystallographic a-axis direction and c-axis direction are indicated. The wavy domain boundary is seen at the center. The left-hand side is the strained domain, and the right-hand side is the monoclinic phase.

very weak at the beginning, but it can be observed very clearly around 170 K, and it becomes stronger at last. The onset temperature of the appearance of this asymmetry is uncertain. Detection of onset temperature may be possible by quantitative measurements of intensity in CBED patterns. However, in the present experiment, intensities were not measured. According to the results by x-ray diffraction, this transition to the monoclinic lattice takes place around 240 K, and on cooling the increase in the angle β from 90° is observed, and it becomes 90.05° around 170 K. Since CBED patterns can be taken within a region less than 10 nm, in following observations we used this technique to identify the crystal lattice type of nano-domains in TEM images.

On cooling to 140 K, new domains with lattice strain contrast appear in images of electron microscope. This temperature is slightly lower than the T_{MI} obtained by x-ray diffraction in Fig. 1. Below this temperature, growth of the new domains is observed on cooling. Figure 4 indicates the coexistent state of two kinds of domains with clear boundaries observed at the [001] zone axis direction at 110 K. The new domains show lamella or layered shape. The matrix seen in the lower part in Fig. 4 is identified as a monoclinic phase by CBED. Crystallographic structure in the lamella domains was unknown, since CBED patterns were very much distorted due to a strong local lattice strain inside the domains. According to the x-ray diffraction experiment, the two-phase state consisting of the monoclinic and LTO phases appears in this temperature region. Thus the layered domains with high strain seen in Fig. 4 should be the LTO phase, or they may include the LTO phase with the monoclinic phase.

Figure 5 shows two kinds of domains observed at the [010] zone axis direction in the specimen for $x=0.39$ at 110 K. The wavy domain boundary at the center separates a domain with strain seen at the left-hand side from the monoclinic domain with no strain contrast on the right-hand side in this figure. A domain at the left-hand side is accompanied by fine strain contrast. Figure 6 shows an observed result at the [100] zone axis direction at 110 K. Below 140 K on cooling, growth of domains with high-strain contrast was observed. The domain, which is located at the lower part of
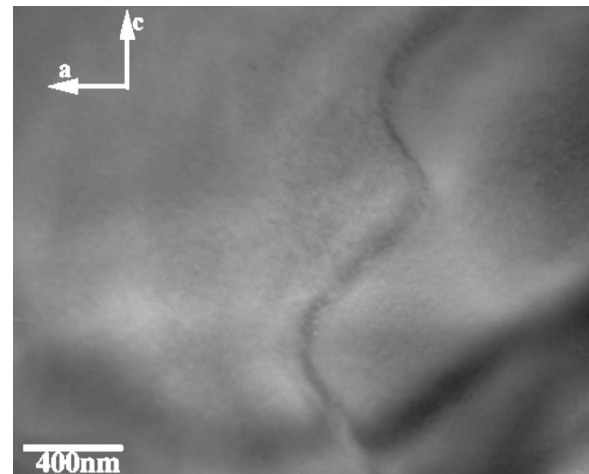
the figure without strain contrast, was confirmed to be a monoclinic phase by CBED. The crystallographic structure with wavy strain contrast seen in the upper part remains uncertain because of the strong local strain. The strain contrast of the domain at the [100] zone axis appears more strongly than that observed at the [010] zone axis. Similar high-strained phases with the wavy and tweed pattern contrast seen in Fig. 6 have been often reported and discussed in various systems.[18–23] It is not certain whether the origins of those strain contrasts are the same or not.

The nanodomain structure shown in Fig. 7 is often observed in the monoclinic phase at the [100] zone axis direction. This photograph was taken at 110 K. Boundaries of
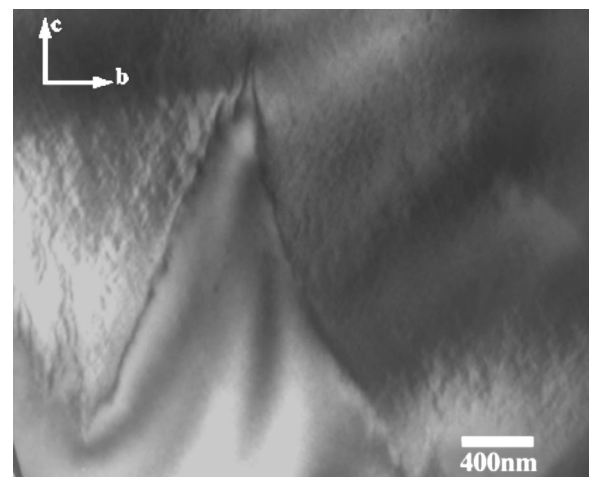

FIG. 6. Electron microscope image at the [100] zone axis direction taken at 110 K of the specimen for $x=0.39$. The domain with high strain and wavy contrast is visible at the upper part. The lower domain without strain and wavy contrast was identified as a monoclinic phase by CBED pattern.

FIG. 7. Nanodomain structure observed at the [100] zone axis direction of the specimen for $x=0.39$ in the monoclinic phase at 110 K.

these domains tend to lie on the *a-b* plane, while those on the *a-c* plane cannot be clearly observed, and lattice strain contrast is accompanied at such uncertain boundary. The onset temperature of the appearance of these domain boundaries is uncertain, since the contrast is very weak at the beginning. However, it becomes stronger on cooling. A reversal of the asymmetry in the CBED patterns was observed around these domain boundaries. Thus, we concluded that these are twin domains of the monoclinic lattice. We noticed that fine and multiple twin structures of the monoclinic lattice exist around the high-strained domains in the phase separated structure.

In the insulator specimen for $x=0.37$, the twin structure of monoclinic lattice similar to Fig. 7 appears on cooling. The state of coexistence of two kinds of domains seen in Figs. 4–6 was not yet observed down to around 110 K. These agree with the results by the x-ray powder diffraction, seen in Fig. 1.

The specimen for $x=0.41$ should be in the two-phase separated state at room temperature according to the x-ray diffraction experiment seen in Fig. 1. However, such separation was not clearly recognized by the present TEM observation. CBED patterns at room temperature indicate the orthorhombic lattice. The similar images of Fig. 4–7 were all observed in the specimen for $x=0.41$, but they appeared at higher temperatures, about 100 deg higher than the case for $x=0.39$.

By using TEM we could observe the phase separated state in real space, and could obtain agreements with x-ray diffraction results except for some differences in T_{MI}. Reasons for these differences are unknown. However, some possibilities for these differences will be discussed in part of the following section. Also, the shapes of the domains as well as possible origins of the high-strain contrast in images of phase-separated state will be discussed.

III. DISCUSSION

The two-phase separation itself will be described by the standard thermodynamic argument, see Secs. 4.2 and 4.3 of Ref. 1, for example. The free energy curves as functions of
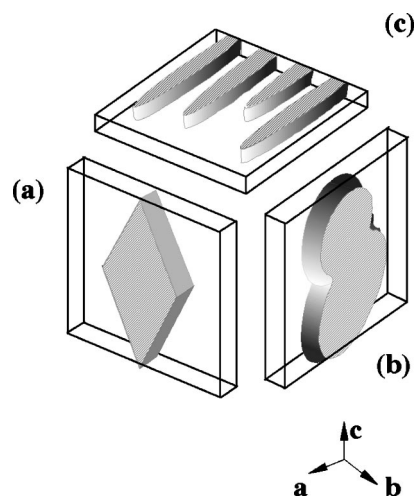

FIG. 8. Different shape of domain boundaries in thin films viewed from three principle axes. (a) The observation direction is the [100] zone axis. The domain boundary takes a zigzag pattern, or diamond-shape elongated to the c-axis direction. (b) The [010] zone axis direction, rounded shape, and (c) the [001] zone-axis direction, the lamella or layer structure.

hole or *d*-electron density for two phases should have local minimums or positive second-derivatives at the vicinity of MI transition. Then, a common tangential line, which contacts both free energy curves at two different points for two phases, can be drawn in the diagram of free energy curves. The two-phase separation takes place in a hole density region between the two contact points. By this separation discontinuous increase in hole concentration in a local domain takes place, and the metallic state appears.

In YTiO$_3$, the bond-angles of Ti-O-Ti are regarded to be 140° on the *ab* plane and 144° along the *c* axis.[7,9] This lattice distortion causes a narrow bandwidth W for the Ti-3d electron state,[7,9] but Ca doping introduces the relaxation of the lattice distortion. According to the lattice parameter measurement by x-ray diffraction,[4] the ratios for *a*, *b*, and *c* axes change toward $\sqrt{2}:\sqrt{2}:2$ by the Ca doping, indicating that lattice structure is approaching cubic, and an increase in the bond angles of Ti-O-Ti takes place. As a result the broadening of the Ti-3d bandwidth W will be expected. Then, the condition for the transition to a metallic state is reinforced. Ca doping introduces not only the band filling control[7,11] but also the bandwidth control, and lattice strain may play an important role.

We have made three different shaped specimens for the [100], [010] and [001] zone axes observation by TEM. The specimen for observation at the [100] zone axis direction was thin films of about several tens of nanometers in thickness along this direction for the electron transparency. Specimens for [010] zone axis and [001] zone axis observations were also of similar thickness. The observed domains showed different shapes depending on observation directions. At the [100] zone axis observation, the domain boundary takes a diamond-shape elongated toward the *c*-axis direction or complex shapes with zigzag pattern as seen in Fig. 6. On the other hand, as seen in Fig. 5, nearly round-shaped domain boundary is observed at the [010] direction. The clear

lamella or layer structure was seen at the [001] zone axis observation in Fig. 4. The schematic views are presented in Fig. 8. The boundaries of these domains as well as the domain itself, may be accompanied by strong stress, and in thin film specimens, lattice stress can relax partly along the normal directions of the film surface, see, for example, Ref. 24. Therefore, the boundaries may take shapes in such ways to reduce the total energy depending on both shapes of the specimens and elastic anisotropy. The differences in appearance at three observation directions may be concluded to be caused by the stress relief effect by surface. The powder specimens for x-ray diffraction are of several micrometers in radius, and they are larger than the thickness of TEM specimens, thus the domains in powder specimens may have different shapes from those observed by TEM.

In the specimen for $x=0.41$, the phase separated state was not observed clearly at room teperature, regardless of the presence of the two-phase state by x-ray diffraction. As one of the possibilities there may be a small difference in chemical composition between the x-ray powder specimen and the TEM specimen. However, let us consider the case of the same composition.

In this system, it is reported that an application of pressure by 0.41 GPa is equivalent to the substitution of Ca by $x=0.01$, and in both cases transition temperature T_{MI} rises.[16] Oppositely, a release of the pressure decreases T_{MI}. In thin film specimens as we have discussed above, a release of built-in stress may take place, as well as a decrease of T_{MI}. Differences in measured strained state between x-ray and electron microcopy are often reported in analysis of semiconductor artificial heterostructures, and these are discussed to be a relief of built-in stress in thin films for TEM observation, see for example the introduction of Ref. 25. The stress relief effect in thin film might be the reason why the phase separation at room temperature was not observed in the specimen for $x=0.41$ by TEM. For $x=0.39$ the phase separation was observed below the x-ray diffraction results by approximately $\simeq 10-20$ deg. This difference also may be caused by the stress relief effect in thin films.

The high-strained domains observed at low temperature seen in Figs. 4–6 might be caused by an introduction of strain in thin films due to the relief of built-in stress which may be inside the LTO phase, as one possibility. The appearance may suggest the presence of characteristic built-in stress in LTO phase in bulk crystals. However, it is not sure that the high-strain contrast is completely attributed to the stress relief effect. Let us consider another possibility also, a case where the high-strained state is not due to the stress relief effect, but an inherent structure for the LTO phase even in bulk. The modulation structure with high-strain indicates the presence of local fluctuation in bond angles, interatomic distances and maybe Ti-3d electron concentration as well. There appear more than two stable local densities of Ti-3d electrons in the phase separated structure. By the phase rule, fluctuations of other parameters, such as the ordering parameter of spin, orbital, etc., may be present at the same time, as well as the fluctuations of Ti-3d density. This is a more complicated situation than the simple thermodynamic model of two-phase separation described at the beginning of this section.

Horibe and co-workers have observed similar phase separation accompanied with domains of high strain and modulation of lattice at low temperatures by TEM in La$_{1.5}$Sr$_{0.1}$Nd$_{0.4}$CuO$_4$ and related compounds.[19–21] A specific time-dependent appearance of the phase separation was explained by a model in which both the phase separation and appearance of high-strained state reduce the free energy of the system. Namely, fluctuations of two parameters were introduced. One is the local ordering parameter for strain and modulation. The other is the local electron density. The appearances of the phase separation and high strained state observed in their compounds are similar to the present results except for the time-dependent behavior.

Recently, many examples of phase separations in manganese oxides have been reported.[26–35] The electrical phase separations by charge ordered domains were observed at low temperatures at the compositional boundary between ferromagnetic metals and anti-ferromagnetic insulators. These phenomena are explained assuming double exchange interaction based on the exchange of an electron between Mn^{3+} and Mn^{4+}.[35] In the present Ti oxide with one t_{2g} electron, the double exchange interaction is not concerned. YTiO$_3$ is ferromagnetic with an orbital ordering due to the super-exchange interaction below $T_c=30$ K.[36,37] Therefore, exchange interaction, and ordering parameters for orbital and spin might also play a role as well as the hole concentration by Ca doping around $x\simeq 0.37-0.41$.

In the metallic region at the vicinity of the temperature-induced insulator-to-metal transition of Y$_{1-x}$Ca$_x$TiO$_3$ at $x \simeq 0.37-0.41$, various physical properties have been measured, such as electrical resistivity,[5,16] electronic specific-heat,[5] photoemission spectra,[10] and so forth. These results should be understood as averaged properties of the different phases in the separated state.

IV. SUMMARY

To summarize, present TEM observation has indicated structural changes in Y$_{1-x}$Ca$_x$TiO$_3$ ($x=0.37$, 0.39 and 0.41) during the transition from an insulator to a metal. In the specimen for $x=0.39$, on cooling, a transition from orthorhombic to monoclinic lattice was confirmed clearly at 170 K. The state of two kinds of domains coexistence appeared at 140 K around the insulator to a metal transition temperature. This is the phase separated state as described in the x-ray diffraction results. In the insulating specimen $x=0.37$, the appearance of the monoclinic lattice was observed, but the phase-separated state was not observed down to 110 K. By the x-ray diffraction the phase separation appears at room temperature for specimen $x=0.41$, however, the phase separation was not observed by TEM. On cooling the phase separation was observed. Details of the mechanism and the relationship between these complicated structural changes and the MI transition remain to be studied further. This is the first report on TEM observation of the electrical phase separation associated with the metal-insulator transition in paramagnetic Y$_{1-x}$Ca$_x$TiO$_3$.

*Electronic address: h.matsuhata@aist.go.jp

[1] N. F. Mott, *Metal-insulator Transition*, 2nd ed. (Taylor and Francis, London, 1990).

[2] S. A. Carter, T. F. Rosenbaum, P. Metcalf, J. M. Honig, and J. Spalek, Phys. Rev. B **48**, 16841 (1993); G. S. Thomas, D. H. Rapkine, S. A. Carter, A. J. Millis, T. F. Rosenbaum, P. Metcalf, and J. M. Honig, Phys. Rev. Lett. **73**, 1529 (1994).

[3] K. Kumagai, T. Suzuki, Y. Taguchi, Y. Okada, Y. Fujishima, and Y. Tokura, Phys. Rev. B **48**, 7636 (1993).

[4] Y. Taguchi, Y. Tokura, T. Arima, and F. Inaba, Phys. Rev. B **48**, 511 (1993).

[5] Y. Tokura, Y. Taguchi, Y. Moritomo, K. Kumagai, T. Suzuki, and Y. Iye, Phys. Rev. B **48**, 14063 (1993).

[6] T. Katsufuji and Y. Tokura, Phys. Rev. B **50**, 2704 (1994).

[7] T. Katsufuji, Y. Taguchi, and Y. Tokura, Phys. Rev. B **56**, 10145 (1997).

[8] Y. Tokura, J. Phys. Chem. Solids **53**, 1619 (1992).

[9] Y. Okimoto, T. Katsufuji, Y. Okada, T. Arima, and Y. Tokura, Phys. Rev. B **51**, 9581 (1995).

[10] K. Morikawa, T. Mizokawa, A. Fujimori, Y. Taguchi, and Y. Tokura, Phys. Rev. B **54**, 8446 (1995).

[11] M. Imada, A. Fujimori, and Y. Tokura, Rev. Mod. Phys. **70**, 1039 (1998).

[12] J. Zaanen, G. A. Sawatzky, and J. W. Allen, Phys. Rev. Lett. **55**, 418 (1985).

[13] F. Iga, T. Nishiguchi, and Y. Nishihara, Physica B **206–207**, 526 (1996).

[14] F. Iga, T. Naka, T. Matsumoto, N. Shirakawa, K. Murata, and Y. Nishihara, Physica B **223–224**, 526 (1996).

[15] K. Kato, E. Nishibori, M. Takata, M. Sakata, T. Nakano, K. Uchihira, M. Tsubota, F. Iga, and T. Takabatake, J. Phys. Soc. Jpn. **71**, 2082 (2002).

[16] M. Tsubota, F. Iga, T. Nakano, K. Uchihira, S. Kura, M. Takemura, Y. Bando, K. Umeo, T. Takabatake, E. Nishibori, M. Takata, M. Sakata, K. Kato, and Y. Oishi, J. Phys. Soc. Jpn. **72**, 3182 (2003).

[17] D. B. Williams and C. B. Carter, *Transmission Electron Microscopy* (Plenum, New York, 1996).

[18] T. Onozuka, N. Ohnishi, and M. Hirabayashi, Metall. Trans. A **19**, 797 (1988).

[19] Y. Horibe, Y. Inoue, and Y. Koyama, J. Supercond. **10**, 461 (1997).

[20] Y. Inoue, Y. Horibe, and Y. Koyama, Phys. Rev. B **56**, 14176 (1997).

[21] Y. Horibe, Y. Inoue, and Y. Koyama, Phys. Rev. B **61**, 11922 (2000).

[22] A. M. Bratkovsky, V. Heine, and E. K. Salje, Philos. Trans. R. Soc. London **354**, 2875 (2000).

[23] Y. Yamada, T. Iwase, K. Fujishiro, Y. Uesu, Y. Yamashita, I. Tomeno, and S. Shimanuki, Ferroelectrics **240**, 363 (2000).

[24] Anisotropic stress relief can take place by the surface effect for thin film specimens with built-in stress inside. However, the following articles are not for the case of electrical phase separation, but for a case of semiconductors hetero-structure. D. Cherns and A. R. Preston, J. Electron Microsc. Tech. **13**, 111 (1989); U. Bangert and P. Charsley, Philos. Mag. A **59**, 629 (1989); D. D. Perovic and G. C. Weatherly, Ultramicroscopy **35**, 271 (1991); H. Matsuhata, K. Miki, K. Sakamoto, T. Sakamoto, and S. Yoshida, Phys. Rev. B **47**, 10474 (1993).

[25] D. D. Perovic, G. C. Weatherly, and D. C. Houghton, Philos. Mag. A **64**, 1 (1991).

[26] C. H. Chen and S-W. Cheong, Phys. Rev. Lett. **76**, 4042 (1996).

[27] S. Mori, C. H. Chen, and S-W. Cheong, Phys. Rev. Lett. **81**, 3972 (1998).

[28] P. G. Radaelli, D. E. Cox, M. Marezio, and S-W. Cheng, Phys. Rev. B **55**, 3015 (1997).

[29] S. Mori, C. H. Chen, and S-W. Cheong, Nature (London) **392**, 473 (1998).

[30] S. Mori, T. Katsufuji, N. Yamamoto, C. H. Chen, and S-W. Cheong, Phys. Rev. B **59**, 13573 (1999).

[31] Y. Moritomo, A. Machida, S. Mori, N. Yamamoto, and A. Nakamura, Phys. Rev. B **60**, 9220 (1999).

[32] R. Kajimoto, H. Yoshizawa, H. Kawano, H. Kuwahara, Y. Tokura, K. Ohoyama, and M. Ohashi, Phys. Rev. B **60**, 9506 (1999).

[33] M. Uehara, S. Mori, C. H. Chen, and S-W. Cheong, Nature (London) **399**, 560 (1999).

[34] A. Machida, Y. Moritomo, E. Nishibori, M. Tanaka, M. Sakata, K. Ohyama, S. Mori, N. Yamamoto, and A. Nakamura, Phys. Rev. B **62**, 3883 (2000).

[35] A. Moreo, S. Yunoki, and E. Dagotto, Science **283**, 2034 (1999).

[36] J. R. Hester, K. Tomimoto, H. Noma, F. P. Okamura, and J. Akimitsu, Acta Crystallogr., Sect. B: Struct. Sci. **53**, 739 (1997).

[37] H. Ichikawa, J. Akimitsu, M. Nishi, and K. Kakurai, Physica B **281–282**, 482 (2000).